

Guiding the Selection of Novel Amines for CO₂ Capture Using a Molecular-Based and Multicriteria Modeling Approach

Published as part of *Energy & Fuels* special issue "Celebrating Women in Energy Research".

Fareeha Shadab, Ismail I. I. Alkhatib, and Lourdes F. Vega*



Cite This: *Energy Fuels* 2024, 38, 17805–17821



Read Online

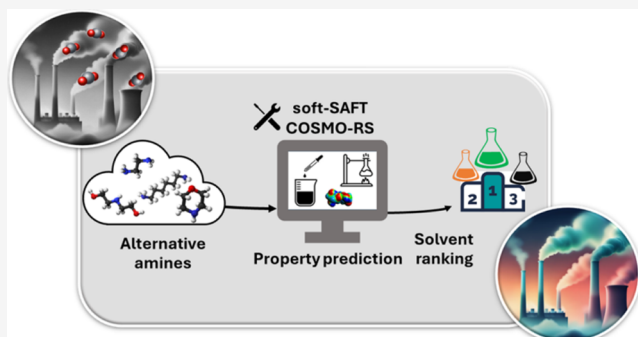
ACCESS |

Metrics & More

Article Recommendations

Supporting Information

ABSTRACT: Given the variety of novel amines as potential next-generation solvents for CO₂ capture, knowledge of their thermodynamic properties is imperative to guiding their selection. In this work, 37 alternative amines belonging to different molecular families are investigated using the soft-statistical associating fluid theory (soft-SAFT) molecular equation of state (EoS). Limited experimental data of density, vapor pressure, and viscosity were used in parametrizing the molecular models, relying on the transferability of parameters related to their functional groups, yielding a modeling accuracy of within 10% of available data. The physical basis of soft-SAFT allowed determining the role of carbon chain length, molecular geometry, and degree of functionalization on key properties for CO₂ capture including density, vapor pressure, heat capacity, heat of vaporization, and viscosity, identifying short-chain molecules with cyclic/branched structures and secondary or tertiary amine functional groups as more preferred. pK_a values were obtained from COSMO-RS as a measure of the affinity for CO₂, establishing the imperative role of functionalization with primary and secondary amine groups. The cost and flammability of the alternative solvents were also included as additional criteria for their final selection. In addition to quantifying the role of the molecular structure on the performance of the solvents, the methodology of this work allowed us to identify morpholine (Morph) and ethylenediamine (EDA) as potential next-generation CO₂ capture solvents, with superior performance to the current ones, to be further investigated for large-scale validation. This work showcases the relevance of using molecular modeling for systematic screening of novel solvents for CO₂ capture, even in the absence of experimental data.



1. INTRODUCTION

The severity of climate change is escalating with the rapid increase in atmospheric CO₂ emissions, inching to their record-breaking high over the past centuries, calling for immediate actions.¹ The United Nations' Sustainable Development Goal 13 (UN-SDG-13) highlights the pivotal role of climate action for achieving net-zero emission pledges by 2060–2070. In similar efforts, the 2030 agenda for sustainable development calls for a 45% reduction in CO₂ emissions by 2030 from their 2010 levels, while pushing the wheel toward carbon neutrality by 2050, to keep global temperatures within the 1.5 °C limit of the Paris Agreement.²

Climate change has been aggravated by the large industrial dependency on fossil fuels as primary energy resources with their high contribution to global CO₂ emissions (~40% of total emissions).³ Although shifting the energy nexus toward dependency on renewable resources or enhancing the energy efficiency of the system are possible solutions to curb the increasing CO₂ emissions, they remain challenged by technical barriers such as high investment costs and intermittency impeding their benefits on short or medium terms. Therefore,

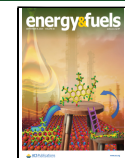
developing sustainable strategies such as carbon capture, utilization, and storage (CCUS) value chain is crucial to reducing CO₂ emissions in the interim stage. With the global race toward net-zero emissions by 2050, the global CO₂ capture capacity must increase by 20 times to meet the 2030 target of capturing 840 million tons CO₂ per year.⁴ Additionally, the investment environment is supportive of deploying CCUS technologies, as governments and industries have committed more than \$25 billion to fund the deployment of new CCUS facilities and research and development projects to enhance their technology readiness level.⁵ However, the upfront investment costs for CCUS remain economically challenging, as the carbon capture stage is the most cost-

Received: July 2, 2024

Revised: August 21, 2024

Accepted: September 4, 2024

Published: September 11, 2024



intensive stage, accounting for 70% of the overall investment costs.^{6,7}

Over the past few years, several technologies for CO₂ capture and separation have been developed, such as absorption via solvents, adsorption via solids, membrane separation, cryogenics, and other novel technologies.⁸ Among them, CO₂ absorption using aqueous amine solvents remains the most commercially viable and mature option today,^{9,10} due to its long-standing history since the 1960s for natural gas sweetening process,⁸ its efficiency and low cost versus others. With this technology, CO₂ is absorbed from incoming flue gas streams at low pressures and temperatures, through forming weakly bonded reaction intermediates between the captured CO₂ and the amine molecule. The solvent is regenerated through the application of heat to recover the captured CO₂ that can be subsequently stored or further utilized in other industries for the creation of value-added products.^{8,11} Nonetheless, this technology is hindered from being used at the required large scale because of its high energy costs required for solvent regeneration, related to heat and vaporizing the large quantities of water in the solution (i.e., latent and sensible heats), and overcoming the chemical bonds formed during the absorption process (i.e., absorption enthalpy), largely dependent on the structure of the amine molecule.¹² For example, the golden-standard solvent, 30 wt % aqueous monoethanolamine (MEA) has a high regeneration energy, accounting for 57% of its total energy consumption.⁸

Overcoming this hurdle has opened the path for a variety of potential alternatives, including water-lean,^{13–16} and water-free solvents,^{17,18} CO₂ organic binding liquids,¹⁹ biphasic amines,^{20,21} task-designer solvents,^{20,22,23} and others, with attractive properties for CO₂ capture, yet still in the early development stage for large-scale postcombustion capture (PCC), leaving the hunt for alternative aqueous amines ongoing.^{24,25}

A wide range of alternative amine molecules have been developed for CO₂ capture,^{8,26–28} yet, the selection of an effective solvent is a cumbersome task due to inherent trade-offs between their preferred properties such as uptake capacity, regeneration energy, stability, kinetics, and viscosity. These properties are largely dependent on the molecular structure of the amine molecule (i.e., type of amine group, other functional groups, carbon backbone chain length, etc.) directly affecting the affinity of the solvent to CO₂ and subsequent energy required for its desorption and capture cost.²⁹ These structural variations gave rise to a diversity of structural functionalities and, hence, alternative amines to be tested, including cyclic, sterically hindered, polyamines, and many others. For instance, Chowdhury et al.,³⁰ investigated the CO₂ absorption performance of several amines with different functional group placements in linear carbon backbones, such as 2-(isopropylamino)ethanol (IPAE), 2-(isobutylamino)ethanol (IBAE), 1-methyl-2-piperidineethanol (1M-2PPE), and 2-(isopropyl)diethanolamine (IPDEA), demonstrating the profound effect of strategically placing the amine functional group and alkyl branch on enhancing absorption capacity and resistance to degradation. Singh et al.,^{31,32} investigated the effects of the carbon backbone chain length and types of different functional groups such as hydroxyl (−OH) group, alkyl-amine, and diamines within the primary amine structure, revealing the effects of activating bulky groups with additional chemical functionalities on increasing absorption capacity and improved stability. Similarly, Conway et al.,³³ proposed a series

of designer amines based on two cyclic skeletal structures, determining that the introduction of various substituents such as hydroxyl groups and additional amine groups around the cyclic ring structure can lead to solvents with superior performance compared to MEA. Li et al.,³⁴ developed a new heterocyclic amine 4-aminomethyltetrahydropyran (4-AMTHP) with superior performance to the benchmark MEA. Moreover, the success of developing solvent blends combining the benefits of primary and secondary amines, as an example, into the same solution has opened the door to developing polyamine solvents with both functionalities embedded in a single molecule such as, N-methyl-1,3-propanediamine (MAPA), diethylene-triamine (DETA), and pentamethyl-divinyl-triamine (PMDETA).^{35–37}

In spite of the pioneering work in developing alternative amine solvents just mentioned, much work is still needed to advance in the development and testing of efficient novel absorbents.^{38–43} At this stage, the key to guiding the development and deployment of promising solvents is the molecular-level understanding on the solvent's microscopic characteristics and their relation to macroscopic behavior. Considering the wide array of solvents recently developed, such a fundamental level understanding requires the implementation of reliable paradigms based on molecular modeling tools as a time- and cost-efficient approach complementary to standard experimental techniques. One commonly employed model is the statistical associating fluid theory (SAFT) equation of state (EoS). Several works in the literature have explored the implementation of SAFT-based models such as SAFT- γ Mie GC,⁴⁴ SAFT-VR,^{45–47} PC-SAFT,⁴⁸ and cubic-plus-association (CPA),^{49,50} for studying the behavior of aqueous amine solvents + CO₂ mixtures, exploring conventional solvents such as cyclic amines, alkyl polyamines, and alkanolamines. Similar works have been done using the soft-SAFT EoS,⁵¹ focusing on conventional aqueous amines and blends, and water-free solvents,^{52–56} developing the basis for a solvent screening tool. Other approaches have been adopted in the literature such as those relying on machine learning,^{57–61} though innovative, still, rely on the availability of comprehensive data sets for high modeling accuracy, which are unavailable for novel systems, highlighting the value of thermodynamic models with strong physical basis.

In this contribution, we extend the application of the solvent screening tool using soft-SAFT as a reliable platform to assess for the first time the performance of next-generation alternative amine molecules for large-scale carbon capture.^{54,55,62} To this end, coarse-grain molecular models for 37 amine molecules belonging to a variety of molecular families (i.e., linear monoamines, cyclic monoamines, linear diamines, cyclic diamines, and linear polyamines) are characterized using available experimental data to build robust molecular models descriptive of their key molecular features. These molecules are chosen based on an exhaustive literature search for solvents either already available in the market or extensively examined on lab-scale, provided availability of experimental property data. The models are used to quantify the effects of microlevel precursor (i.e., structure, chain length, number, and type of functionalities) on key properties for CO₂ capture, as well as to predict macroscopic properties at industry-relevant conditions. The predicted properties, and additional properties, such as flammability and cost, are subsequently used in a multicriteria analysis framework using statistical methods to rank the best-performing amine molecules for additional future evaluation.

2. METHODOLOGY

2.1. Soft-SAFT Equation of State. The soft-SAFT EoS used in this work, introduced by Blas and Vega in 1997,⁵¹ belongs to the SAFT-family of molecular-based EoSs. Soft-SAFT is written in terms of the residual Helmholtz free energy (a^{res}) of a fluid as the sum of contributions, taking into account the structure of the molecules integrating the fluid

$$a^{\text{res}} = a^{\text{ref}} + a^{\text{chain}} + a^{\text{assoc}} + a^{\text{polar}} \quad (1)$$

with a^{ref} denoting the reference term for the attractive and repulsive interactions between individual Lennard-Jones (LJ) segments forming the molecules, a^{chain} denoting the chain term representing chain formation from connected individual segments, and a^{assoc} denoting the association term representing contribution from highly directional and localized interactions such as the formation of hydrogen bonds between different molecules or different functional groups on the same molecule. a^{ref} is calculated using Johnson et al.,⁶³ while a^{chain} and a^{assoc} , formally identical across all SAFT-based models, derived by Chapman et al.,^{64,65} from Wertheim's first-order thermodynamic perturbation theory (TPT1).^{66–69} Lastly, a^{polar} denotes the polar term explicitly accounting for permanent dipole or quadrupole interactions, written based on the theory of Gubbins and Twu^{70,71} for spherical molecules, and its extension to chainlike fluids by Jog and Chapman.^{72,73} Additional details on these terms can be found in the original works.^{51,74}

The decision of choosing soft-SAFT over other SAFT models for this work is primarily due to the demonstrated accuracy in describing solvents for CO₂ capture, building on the existing work in the area.^{52–56} Other SAFT-based models might result in a similar level of accuracy; however, a comparison of them is outside the scope of this work.

A coarse-grain (CG) molecular model for the fluid representative of its molecular features (i.e., structure and energy), captured by a set of molecular parameters, is required to apply the soft-SAFT EoS. The three basic nonassociating molecular parameters, irrespective of fluid type, are the chain length (m), LJ segment diameter (σ), and dispersive energy (ϵ). For associating fluids capable of forming hydrogen bonds, two additional parameters are required, aside from the number and type of association sites, including association energy (ϵ^{HB}) and volume (κ^{HB}). Similarly, for polar fluids, two additional parameters are included, the dipole/quadrupole moment (μ/Q) and the fraction of polar segments (x_p). These parameters are obtained either from simultaneous fitting to available pure fluid saturated liquid density and vapor pressure data or fixed a priori based on a physical argument as in the case for the polar parameters.

With the molecular models for the pure fluids developed and validated, the EoS can be used to directly predict a variety of first- and second-order thermodynamic properties including heat of vaporization (ΔH^{vap}) and isobaric heat capacity (C_p), using thermodynamic derivatives^{75–77} and expressions for the pure fluid ideal gas heat capacity obtained from DIPPR 801 database.⁷⁸

2.2. Viscosity Using Free-Volume Theory. The viscosity of alternative amines can be calculated by coupling the soft-SAFT EoS with appropriate complementary theory, such as FVT,⁷⁹ with the EoS providing thermodynamic variables such as pressure, temperature, and density. According to FVT, the dynamic viscosity of a pure fluid (η) is computed as a sum of

two contributions, the dilute gas term (η_0) which is typically omitted for low vapor pressure fluids,⁵⁶ and the dense-state correction term ($\Delta\eta$), as

$$\eta = \eta_0 + \Delta\eta \quad (2)$$

Characterizing pure fluid using FVT requires three parameters, which are the length parameter of the molecule's structure (L_v), free-volume overlap among the molecules (B), and the proportionality between the energy barrier and the density (α). These parameters are fitted to available experimental viscosity data through deviation minimization compared to computed viscosity at similar conditions.⁵⁶

2.3. Amine Affinity to CO₂ Using COSMO-RS. The quantum chemistry-based model conductor-like screening model for real solvents (COSMO-RS) is used in this work to predict the affinity of the alternative amines toward capturing CO₂. This is done using pK_a as a measure of the amines' affinity, with higher values indicative of higher amine basicity and, hence, higher tendency to solubilize CO₂. The application of COSMO-RS requires the three-dimensional (3D) molecular structure of the amine molecule, built using Turbomole software (TMole X version 19)⁸⁰ and then geometrically optimized at the density functional theory (DFT) level using BP86 functional with def-TZVP basis set, subsequently exported to COSMOthermX to predict the pK_a values of the novel amines. The pK_a of a solute, i , is estimated from the linear free energy relationship (LFER), as

$$pK_a^i = c_0 + c_1(G_i^{\text{ion}} + G_i^{\text{neutral}}) \quad (3)$$

where G_i^{ion} and G_i^{neutral} are the free energies of the neutral and the ionic compounds, and c_0 and c_1 are the LFER parameters from the default COSMOtherm parameter file.

2.4. Multicriteria Assessment of Promising Alternative Amines. Considering the large number of alternative amines examined in this work and the inherent trade-offs between their properties of interest for CO₂ capture provided in Table 1, we opted to conduct a multicriteria assessment

Table 1. Summary of Evaluation Criteria for Alternative Amines, Their Intended Variation, and the Assessment Method

criteria	variation	assessment method
density (ρ)	maximized (+)	soft-SAFT
vapor pressure (p^*)	minimized (-)	soft-SAFT
viscosity (η)	minimized (-)	soft-SAFT
heat capacity (C_p)	minimized (-)	soft-SAFT
heat of vaporization (ΔH^{vap})	minimized (-)	soft-SAFT
amine CO ₂ affinity (pK _a)	maximized (+)	COSMO-RS

using a statistical analysis tool, namely, gray relational analysis (GRA) and Technique for Order of Preference by Similarity to Ideal Solution (TOPSIS), to rank and determine most promising amine molecules. Although several alternative techniques are available for multicriteria assessment, GRA and TOPSIS were chosen due to their relative application simplicity, and consistency in translating qualitative data with varying magnitudes into consistent quantitative ranking.^{81,82} Details related to their implementation are provided next, while a more detailed description of the calculation procedure can be found in the original references.^{81,82}

2.4.1. Gray Relational Analysis. GRA is a statistical multiobjective optimization method used to rank the

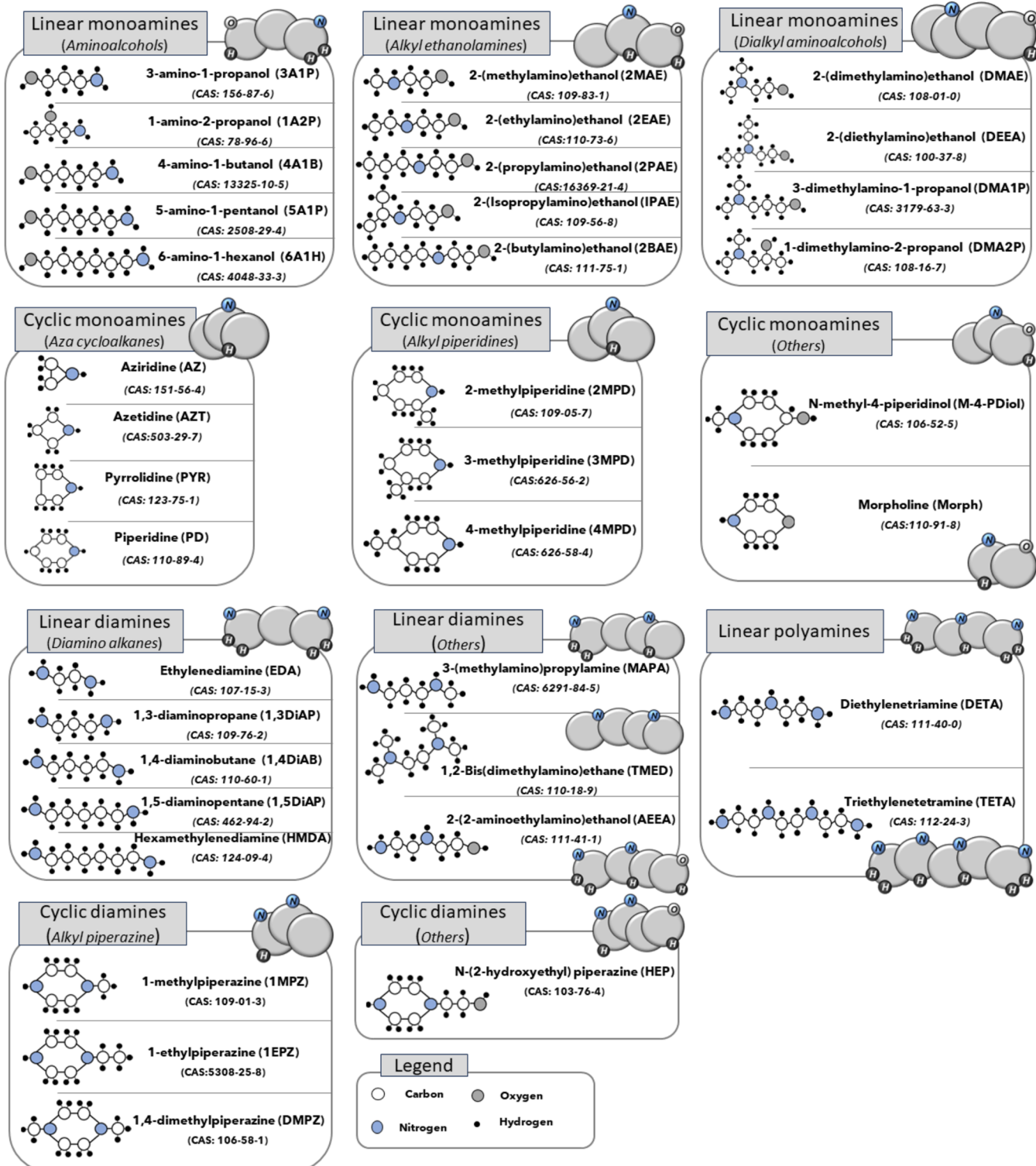


Figure 1. Alternative amines studied in this work with their molecular structure, name, acronym, CAS number, and corresponding soft-SAFT CG molecular models. The color code is provided as a Legend in the figure.

importance of design parameters through their simultaneous optimization.⁸¹ This is applied to rank the different solvents based on their different properties of interest for CO₂ capture.

First, the responses' results (i.e., properties in Table 1) must be normalized between 0 and 1, using the “higher is better” and “lower is better” criteria, based on the desired variation for the property. For example, higher is better if applied for

maximization as with density, while lower is better if applied for minimization as with vapor pressure. Next, the gray relational grade (γ_i) is used as an indicator for solvent ranking, which denotes the level of correlation between the reference and comparative sequences, weighing each thermodynamic property based on its level of importance.

$$\gamma_i = \frac{1}{n} \sum_{k=1}^n \frac{\Delta_i}{\Delta_p} \left(\frac{\Delta_{\min} + 0.5\Delta_{\max}}{(y_o(k) - y_i(k)) + 0.5\Delta_{\max}} \right) \quad (4)$$

where $y_i(k)$ is the property normalized value, Δ_{oi} is the deviation value between $y_o(k)$ and $y_i(k)$, Δ_{\min} and Δ_{\max} are the minimum and maximum values of Δ_{oi} , Δ_i is the deviation value for each parameter, and Δ_p is the sum of Δ_i value for all of the parameters.

2.4.2. Technique for Order of Preference by Similarity to Ideal Solution. TOPSIS is a method that compares a set of alternatives based on a set of criteria, by normalizing scores for each criterion and calculating the geometric distance between each alternative and the ideal alternative, which is the best score in each criterion.⁸³ Similarly, to the GRA method, first, normalization of responses (i.e., properties) is needed, which are given different weights similar to GRA. Next, the relative closeness coefficient (C_i^*), used to rank the solvents, is determined based on the Euclidean distance of each response value from the positive and negative ideal solutions.

$$C_i^* = \frac{D_i^-}{D_i^* + D_i^-} \quad (5)$$

where D_i^* is the positive distance between the weighted response and the ideal positive solution, D_i^- is the negative distance between the weighted response and the ideal negative solution.

3. SOFT-SAFT MODELS FOR THE AMINE MOLECULES

To evaluate the prospect of alternative amine molecules using soft-SAFT EoS, their CG molecular models are required. In this work, a total of 37 different amine molecules (see Figure 1) have been studied belonging to five different categories, namely, linear and cyclic monoamines, linear and cyclic diamines, and linear polyamines.

All of the studied alternative amines have similar CG molecular models, represented as associating chainlike molecules with five molecular parameters (i.e., m , σ , ϵ , ϵ^{HB}/k_B , κ^{HB}), with their corresponding soft-SAFT models included in Figure 1. The primary difference in their models is based on the type and number of association sites dependent on the different functional groups present in their molecular structure.

Linear monoamines are amine molecules with a linear or branched carbon backbone and a single amine group, either primary ($-NH_2$), secondary ($-NH$), or tertiary ($-N$), including the primary aminoalcohols, secondary alkyl ethanolamines, and tertiary dialkyl aminoalcohols.

For aminoalcohols, the presence of $-NH_2$ amine group and the hydroxyl group ($-OH$) at each end of the chain is modeled with five association sites, with three sites for the $-NH_2$ group, two for the hydrogen atoms of type (H), and one for the lone pair of electrons on the nitrogen atom of type (e), and two sites for the $-OH$ group, with one site for the hydrogen atom of type (H) and one site for the two lone pair of electrons on the oxygen atom of type (e). A similar denotation is used for the secondary alkyl ethanolamines and tertiary dialkyl aminoalcohols, with the main difference of having two association sites $-NH$ amine group, one of type H and one of type e, and one association site for the $-N$ amine group of type e, while preserving the number of association sites for the $-OH$ groups.

Cyclic monoamines are akin to linear monoamines in the presence of a single amine group yet with a cyclic structure

rather than linear or branched. For the cyclic aza cycloalkanes and alkyl piperidines, two association sites are added to the model to account for the $-NH$ group, with one site of type e and one site of type H. Special cases include other cyclic monoamines, as with M-4-PDiol, its $-N$ amine group modeled with one association site of type e, and the $-OH$ group with two association sites. In the case of morpholine, aside from the two association sites for the $-NH$ group, an association site of type (e) is added, representing the two lone pair of electrons on the oxygen atom in the ether-like molecule.

Diamines are those molecules with two amine groups in the structure that can be of similar or differing amine groups (i.e., primary, secondary, tertiary) either in a linear or branched structure or cyclic. For linear diamines belonging to the diamino alkane family, the two $-NH_2$ end groups are modeled with six association sites, two of type e for the nitrogen atoms, and four sites of type H for the hydrogen atoms. For other linear diamines, such as TMED, two association sites of type e are included for its two $-N$ groups. For MAPA and AEEA, both molecules possess a $-NH_2$ end group, and a $-NH$ amine group, modeled with a total of five association sites, two sites of type e, and three sites of type H. Additional two sites are added to AEEA to account for its $-OH$ end group.

For the cyclic diamines such as alkyl piperazines as with 1MPZ and 1EPZ, the CG molecular model has three association sites, with one site of type e for the $-N$ group, and two sites for the $-NH$ group with one of type H and one of type e, with the exception for DMPZ, which has two $-NH$ groups, resulting in a two-site model of type e. The model for the cyclic diamine HEP is similar to that for 1MPZ, however, with the addition of two association sites for the additional $-OH$ group.

The models become more complex for polyamines due to the presence of more than two amine functional groups. DETA is modeled with eight association sites, with six of them accounting for the two $-NH_2$ end groups and two sites for the $-NH$ midchain group. Conversely, the most complex model is for TETA, with its four functional groups, two $-NH_2$ groups and two $-NH$ groups, resulting in a total of ten association sites.

To preserve the robustness of the model, it was opted to transfer the values for the association parameters (i.e., ϵ^{HB}/k_B , κ^{HB}) descriptive of the different functional groups from other molecules studied in previous works. The number and type of association sites for the amine molecules modeled in this work are included in Table S1 in the Supporting Information (SI). The association parameters for the $-OH$ group are transferred from ethanol (i.e., $\epsilon^{HB}/k_B = 3386$ K and $\kappa^{HB} = 2641 \text{ \AA}^3$),⁸⁴ the primary $-NH_2$ group are transferred from ethylamine (i.e., $\epsilon^{HB}/k_B = 1695$ K and $\kappa^{HB} = 2000 \text{ \AA}^3$),⁵² the secondary $-NH$ group are transferred from diethylamine (i.e., $\epsilon^{HB}/k_B = 1600$ K and $\kappa^{HB} = 2000 \text{ \AA}^3$),⁵³ and the tertiary $-N$ group is transferred from MDEA (i.e., $\epsilon^{HB}/k_B = 1500$ K and $\kappa^{HB} = 565 \text{ \AA}^3$).⁵³ Note that for morpholine, the ether $-O$ group is treated similarly to the $-N$ group but with higher association energy (i.e., $\epsilon^{HB}/k_B = 2000$ K and $\kappa^{HB} = 565 \text{ \AA}^3$).

In all cases, cross-association interactions between different associating sites on the same molecule (e.g., $OH-NH_2/OH-NH-OH-NH_2-NH/NH_2-N/NH-N/O-NH$) are allowed in the model, only type e-H, predicted from combining rules to compute the unlike-association volume and energy as

Table 2. Soft-SAFT Molecular Parameters and FVT Parameters of the 37 Alternative Amines^a

amine	M_W (g mol ⁻¹)	soft-SAFT parameters			FVT parameters		
		m [-]	σ (Å)	ϵ/k_B (K)	α (J m ³ mol ⁻¹ kg ⁻¹)	10^{-3} B [-]	$10^{-2} L_v$ (Å)
Linear Monoamines (Primary)							
3A1P	75.11	2.459	3.645	329	203.829	9.941	2.694
1A2P	75.11	2.198	3.831	329	203.829	11.267	1.291
4A1B	89.14	2.799	3.735	331	203.829	8.888	10.095
5A1P	103.16	2.849	3.808	335	203.829	8.116	8.747
6A1H	117.15	3.224	3.885	338	203.829	9.366	11.395
Linear Monoamines (Secondary)							
2MAE	75.11	2.247	3.812	308	171.830	11.818	3.563
2EAE	89.14	2.394	3.977	311	171.830	15.483	0.966
2PAE	103.16	2.512	4.130	315	171.830	8.764	21.375
2IPAE	103.16	2.465	4.164	315	171.830	13.397	5.629
2BAE	117.16	2.648	4.258	318	171.830	14.029	3.938
Linear Monoamines (Tertiary)							
2DMAE	89.14	2.289	4.014	273	165.789	12.756	2.203
DEEA	117.19	2.510	4.287	287	144.730	12.257	12.079
DMA1P	103.16	2.442	4.198	349	165.789	6.409	65.804
DMA2P	103.16	2.241	4.243	229	130.579	6.889	47.113
Cyclic Monoamines							
AZ	43.07	2.126	3.235	302			
AZT	57.09	2.160	3.522	303			
PYR	71.12	2.208	3.759	319			
PD	85.15	2.254	3957	327			
2MPD	99.17	2.286	4.205	331	237.809	24.639	27.251
3MPD	99.17	2.355	4.152	331	237.809	24.937	28.639
4MPD	99.17	2.365	4.164	331	237.809	25.133	28.511
M-4PDiol	115.17	2.433	4.202	376	349.000	2.234	22.99
Morph	87.11	2.326	3.813	342	49.469	31.234	66.84
Linear Diamines							
EDA	60.11	2.087	3.690	339	159.658	9.708	3.729
1,3DiAP	74.11	2.313	3.824	345	159.658	12.218	2.174
DAB	88.21	2.505	3.959	351	159.658	14.192	1.000
1,5DiAP	102.21	2.661	4.066	360	159.658	4.879	87.863
HDMA	116.21	2.869	4.167	362	159.658	18.606	0.500
MAPA	88.15	2.659	3.881	320	159.155	8.292	11.332
TMED	116.21	2.365	4.472	325	90.356	8.536	90.030
AEEA	104.15	2.456	4.079	386	177.703	14.946	1.149
Cyclic Diamines							
1MPZ	100.16	2.531	3.982	329	108.677	12.049	28.559
1EPZ	114.19	2.611	4.135	338	108.677	12.575	2.155
DMPZ	114.19	2.583	4.185	320	108.677	9.467	112.8
HEP	130.19	2.671	4.250	348	108.677	33.222	20.901
Linear Polyamines							
DETA	103.17	2.912	3.892	350	127.258	13.765	13.114
TETA	146.23	3.397	4.121	377	115.905	24.032	4.684

^aSee Table S1 in the SI for the number and type of association sites.

$$\kappa_{ab}^{\text{HB}} = \left(\frac{\sqrt[3]{\kappa_a^{\text{HB}}} + \sqrt[3]{\kappa_b^{\text{HB}}}}{2} \right)^3 \quad (6a)$$

$$\epsilon_{ab}^{\text{HB}} = \sqrt{\epsilon_a^{\text{HB}} \epsilon_b^{\text{HB}}} \quad (6b)$$

where κ_a^{HB} , κ_b^{HB} , and ϵ_a^{HB} , ϵ_b^{HB} are the association volume and energy for sites a and b on the molecule.

4. RESULTS AND DISCUSSION

4.1. Thermodynamic Characterization of Pure Alternative Amines Using Soft-SAFT EoS.

Based on the

proposed molecular models of the novel amine molecules and transferability of the association parameters (i.e., ϵ^{HB} , κ^{HB}); only the three nonassociating parameters (i.e., m , σ , ϵ) were optimized (see Table 2) using experimental saturated liquid density and vapor pressure data from the references provided in Table S2 in the SI. Only 50% of the experimental data were used in the parametrization process with the criteria of minimizing the absolute average deviation (AAD%) between the experimental and computed property data. The remaining data were used to test the accuracy of the model for predictions outside the fitting range. The missing data for some of the alternative amines (see Table S2 in the SI) are primarily related to heat of vaporization and isobaric heat

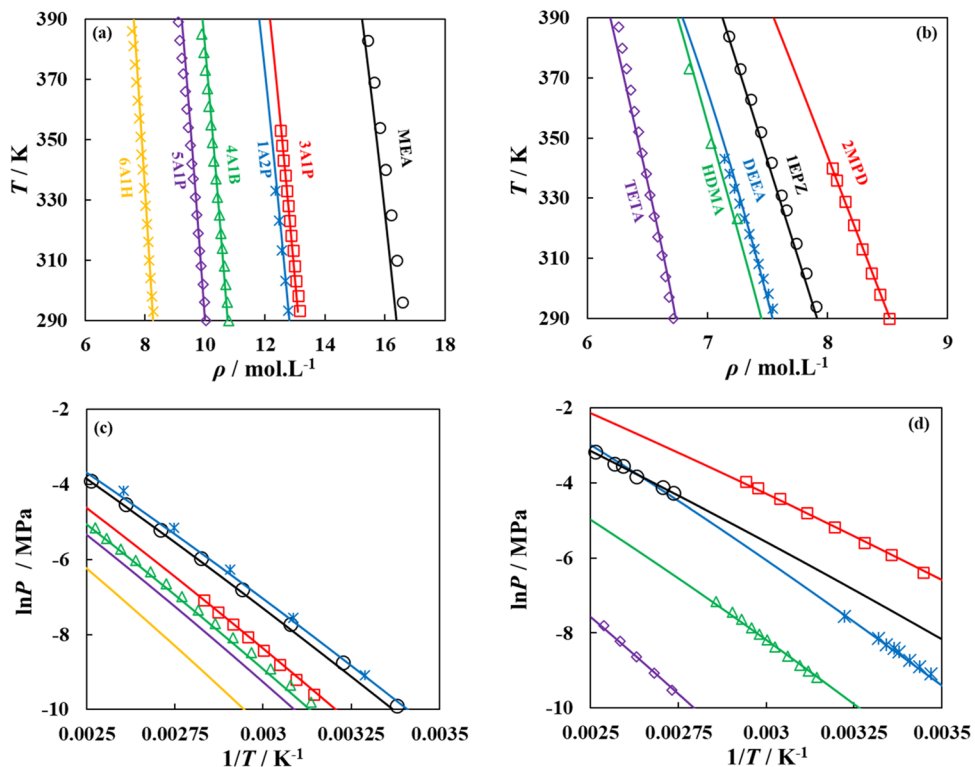


Figure 2. (a) Density for linear monoamine aminoalcohols, (b) density for selected alternative amines with six-carbon chain, (c) vapor pressure for linear monoamine aminoalcohols, and (d) vapor pressure for selected alternative amines with six-carbon chain, with symbols denoting experimental data (see Table S2 in the SI), and lines are soft-SAFT calculations using molecular parameters in Table 2.

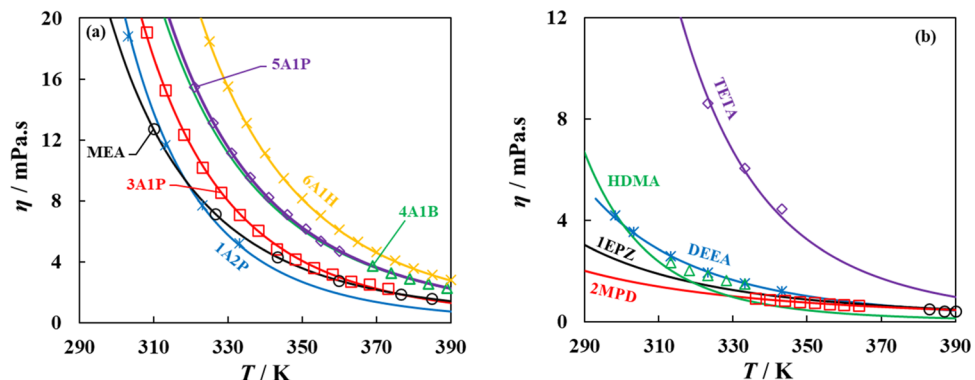


Figure 3. (a) Viscosity for linear monoamine aminoalcohols, and (b) viscosity for selected alternative amines with six-carbon chain, with symbols denoting experimental data (see Table S2 in the SI), and lines are soft-SAFT + FVT calculations using parameters in Table 2.

capacity and do not compromise the model performance, as they are not included in the fitting procedure. For a few cases wherein liquid density, vapor pressure, and viscosity data are missing, the fitting relies on the consistency of the molecular parameter with molecular weight for amines belonging to a homologous series.

The soft-SAFT parameters are used to compute the liquid density and vapor pressure of the alternative amines, and results are provided in Figure 2 for the linear monoamine aminoalcohol (including MEA as the first member of the family with soft-SAFT parameters from previous work)⁵² and selected amines with six-carbon chain from each of the five categories as illustrative examples, while the results for the remaining amines are included in Figures S1 and S2 in the SI.

Excellent agreement between experimental data and soft-SAFT computed properties is seen for all cases, with 0.15 and

2.18% average AAD for the liquid density and vapor pressure, respectively. The minimization of statistical deviation between computed and experimental property data demonstrates the success of the parametrization procedure and the adequacy of the optimized molecular parameters. Additionally, the consistency of molecular parameters reflects the property variation across a single family or different molecules with similar molecular features. This is seen for the linear monoamine aminoalcohols (Figure 2(a)) with the reduction in density with an increasing chain length from MEA (two-carbon chain) to 6A1H (six-carbon chain). Similarly, the density variation for the six-carbon amine molecules from different categories (Figure 2(b)) is reflected with the larger density for cyclic mono- and diamine molecules such as 2MPD and 1EPZ due to their compacted molecular volume in contrast to the lower density for linear diamine and polyamine

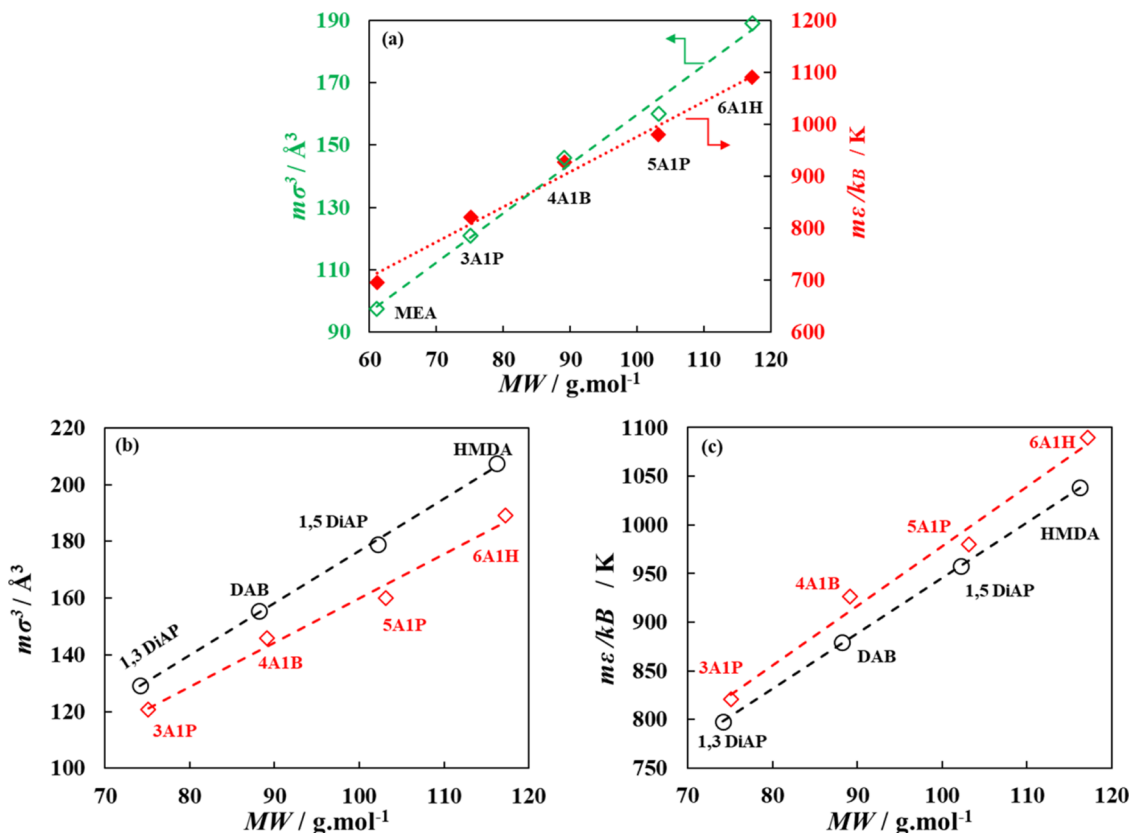


Figure 4. (a) Correlation of the molecular weight with molecular volume (open symbols) and energy (closed symbols) for linear monoamine aminoalcohols, (b) molecular volume trends for linear monoamine aminoalcohols (diamonds) and linear diamine diamino alkanes (circles), and (c) molecular energy trends for linear monoamine aminoalcohols and linear diamine diamino alkanes. Dashed lines are to guide the eyes.

molecules such as HDMA and TETA. This is also reflected for vapor pressure (Figure 2(c,d)) for the same alternative amine molecules, with soft-SAFT capable of effectively capturing the effect of molecular structure and functionality on the change in vapor pressure. Notice that in the case of 5A1P and 6A1H (Figure 2(c)) the vapor pressure was predicted from the model relying on the trend of dispersive energy with molecular weight across the molecular family, highlighting the predictive power of molecular-based EoSs.

For modeling the viscosity of the 37 alternative amine molecules, the FVT parameters were obtained from fitting to available experimental viscosity data (see Table S2 in the SI), by minimizing AAD% deviation between experimental and calculated data. To ensure a robust parametrization process, it was opted to transfer the α parameter across each molecular family, being fixed to the value obtained from the first member of each family, while fitting the remaining FVT parameters (i.e., B , L_v). This was applied, when possible, to linear monoamines from aminoalcohols and alkyl ethanolamines, cyclic monoamine alkyl piperidine, linear diamine diamino alkanes, and cyclic diamines from alkyl piperazine. Alternatively, the three FVT parameters were treated as adjustable parameters and fitted simultaneously to available viscosity data, as in the case of tertiary linear monoamines, linear polyamines, TMED, AEEA, M-4PDiol, and Morph. The optimization procedure for FVT parameters included in Table 2 yielded an average AAD of 1.9% between experimental and computed viscosity data.

The calculated viscosity using soft-SAFT + FVT for linear monoamine aminoalcohols (Figure 3(a)) and selected amines

with six-carbon chain from each of the five categories (Figure 3(b)) is in excellent agreement with the experimental data. Additionally, the optimized parameters enable the model in capturing the change in viscosity for these molecules based on the change in their molecular volumes, with larger viscosities seen for molecules occupying larger volumes due to their high chain length and degree of branching as seen with 6A1H and TETA, compared to smaller viscosities for the more compacted cyclic 1EPZ and 2MPD. Viscosity results for remaining alternative amines using soft-SAFT + FVT are included in Figure S3 in the SI.

An advantage of molecular-based EoSs is the physical meaning of the molecular parameters, allowing the extraction of general trends consistent with the molecular size that permits parameter transferability to other molecules belonging to the same family. These involve investigating the relation of molecular weight (M_W) with the volume of the molecule ($m\sigma^3$) and energy of the molecule ($m\varepsilon$), plotted in Figure 4 for selected families including linear monoamine aminoalcohol and linear diamine diamino alkanes. From Figure 4(a), a nearly linear trend exists between the molecular weight for the aminoalcohol family and their molecular volume and energy, with the correlations included in Table S3 in the SI. The trend increases with increasing molecular weight not only showing the consistency of the optimized molecular volume and energy and their correlativity with molecular weight of the amine molecule ($R^2 > 0.97$), but also capturing the impact of increasing number of carbons in the linear monoamine, from the two-carbon chain MEA to the six-carbon chain 6A1H, on the expansion of the volume occupied by the molecule and its

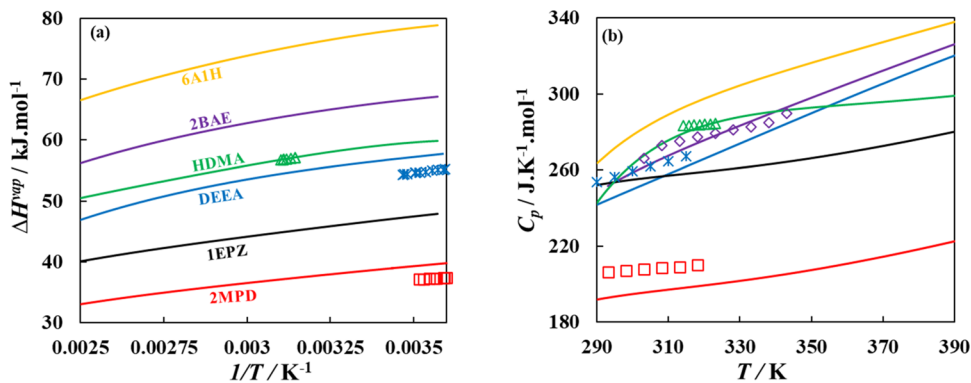


Figure 5. (a) Heat of vaporization (ΔH_{vap}), and (b) isobaric heat capacity (C_p) for selected alternative amines with six-carbon chain, with symbols denoting experimental data (see Table S2 in the SI), and lines are soft-SAFT predictions using parameters in Table 2.

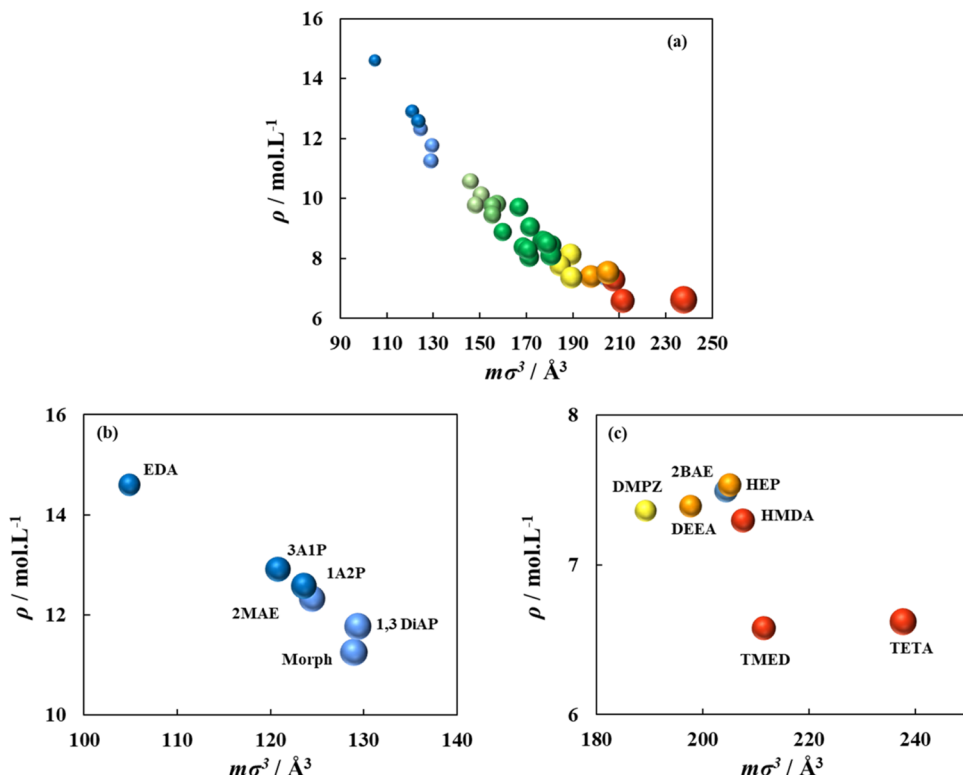


Figure 6. Relationship between liquid density and molecular volume for (a) all alternative amines (color of the sphere denoting molecular volume grading from low (blue) to high (red)), (b) amines with the largest densities, and (c) amines with the lowest densities, as predicted from soft-SAFT at 313 K.

dispersive energy which would consequently impact its volumetric and energetic properties, respectively.

Another example is plotted in Figure 4(b,c), to examine the effect of different functionality seen with aminoalcohols with one primary amine group and a hydroxyl end group, compared with diamines of similar carbon backbone length belonging to diamino alkane family, yet with two primary amine groups. The linearity of the molecular volume with molecular weight in Figure 4(b) supports the consistency of the molecular parameters, as seen across each family. The replacement of the hydroxyl end group with a primary amine group, shifting from an aminoalcohol to a diamine of similar carbon chain length increased the molecular volume, which is attributed to the larger molar mass of the nitrogen atom compared to oxygen atom. Interestingly, the degree of change is relatively small for short chains as seen with 3A1P and its counterpart

1,3 DiAP, yet the jump in molecular volume becomes more pronounced for longer chain molecules as seen with 6A1P and its counterpart HMDA.

The same linearity is also seen for the change of molecular energy with molecular weight for both families in Figure 4(c). However, the molecular energy of aminoalcohols is larger than diamino alkanes, due to the higher electronegativity of the oxygen atom in their OH end group as opposed to the nitrogen atom in the primary amine end group in the diamines.

4.2. Reliability of Soft-SAFT in Predicting Other Properties for Alternative Amines. To test the reliability of the optimized molecular parameters in Table 2, additional properties not included in the parametrization process have been predicted, namely heat of vaporization and molar isobaric heat capacity, presented in Figure 5 for selected amines with

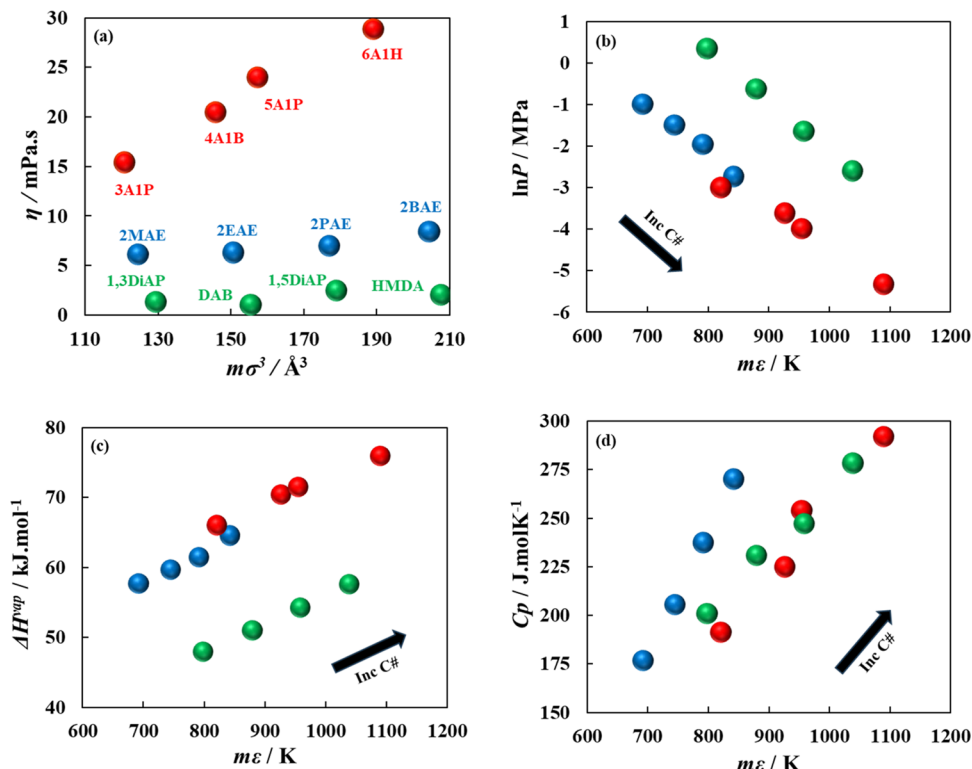


Figure 7. Trends for (a) viscosity with molecular volume, (b) vapor pressure with molecular energy, (c) heat of vaporization with molecular energy, and (d) heat capacity with molecular energy, for aminoalcohols (red spheres), alkyl ethanolamines (blue spheres), and diamino alkanes (green spheres), as predicted from soft-SAFT at 313 K.

six-carbon chain, with results for remaining amines, depending on data availability, in Figures S4 and S5 in the SI.

Note the good agreement between the soft-SAFT predicted property and experimental data, with AAD of 7.2% for enthalpy of vaporization and 6.3% for heat capacity, capturing the correct trend of available experimental data. This gives fidelity in the model to predict these properties for systems in the absence of experimental data as seen in the case of the heat of vaporization for 2BAE, and 6A1H, and the isobaric heat capacity for 1EPZ, and 6A1H. Note that for a few cases (see Figures S4 and S5 in the SI), the agreement is rather qualitative with larger deviations, obtaining correct trends in association with molecular structure. This is expected considering that even small errors in modeling liquid density and vapor pressure tend to propagate with first- and second-order derivative properties. This can be remedied with the inclusion of these properties in the parametrization procedure, however, with increased computational complexity and time. Hence, for the purpose of this work, the obtained accuracy is sufficiently reasonable for a comparative assessment of alternative amine molecules.

4.3. Effect of Structural Functionalities on Fundamental Thermodynamic Properties of Alternative Amines. One advantage of the optimized parameters is the physical meaning linking the microscopic molecular volume ($m\sigma^3$) and energy ($m\epsilon$) of the amines to their macroscopic thermodynamic properties. The chain length, number, and type of functional groups have been shown to affect the properties of amines, often with a certain level of correlation among them.

Shown in Figure 6 is the correlativity of the molecular volume with the density predicted from soft-SAFT at 313 K.

The observable general trend is that density, a volumetric property, is a strong function of molecular volume, with larger molecules tending to have lower liquid densities. The largest density values are seen with short-chain molecules, typically, the first member of the studied families, with the largest densities seen with the two-carbon chain diamine EDA, followed by the three-carbon chain primary monoamine 3A1P and its isomer 1A2P, and three-carbon chain secondary monoamine 2MAE, three-carbon linear diamine 1,3 DiAP, and the four-carbon cyclic monoamine Morph. On the far end of the spectrum, the lowest densities are seen with the larger chain molecules, with the least dense amine being the six-carbon polyamine TETA, and linear diamines HDMA, and TMED, with structural variation.

From the extreme cases, one can argue that the effect of the number of carbons on density is far more pronounced than the number of functional groups or even the geometric structure (i.e., linear, branched, or cyclic). For example, although EDA is a linear diamine, with a two-carbon backbone, its density was higher than short-chain amines with three or four carbons, with the number of carbons being key for controlling the density of the amine molecule, as shown in Figure 6(b). In terms of the geometric structure, the density for the straight chain three-carbon 3A1P was larger than its branched isomer 1A2P, due to the more compacted electron cloud of the latter with the proximity of its hydroxyl group and amine group allowing intramolecular interactions and reduced occupied volume. This effect is also seen with cyclic molecules, although Morph is a four-carbon ring with an epoxy group and a secondary amine, its molecular volume was lower than the three-carbon diamine 1,3 DiAP, with a pronounced role of the geometric structure in reducing the volume occupied by the molecule. Lastly, the

effect of functional groups can be seen in the case of 3A1P and 2MAE, both with three-carbon structures, yet, with the former having a primary amine end group and the latter with a secondary amine group within the carbon chain. The proximity of the secondary amine group to the hydroxyl group can reduce the molecular volume through intramolecular interactions, as seen from the similarity of density between 2MAE and 1A2P.

On the other end of the spectrum, lower densities are seen with larger molecules, as with the six-carbon polyamine TETA and diamine TMED, with a larger volume for TETA on account of its linear structure and the presence of two pairs of primary and secondary amine groups, as opposed to the compacted branched structure for TMED with its two tertiary amine groups. Interestingly, a more pronounced effect for type and placement of functional groups, and molecular geometry can be seen in this case with *Figure 6(c)*, as all of the molecules possess six carbons in their structure.

For example, though HDMA also possessed six carbons in its structure, the absence of the two secondary amine groups compared to TETA reduced its molecular volume as the absence of these groups can allow the molecule to coil without hindrance due to the presence of functional groups with negative repulsive potential within the structure. This is on par with the compacted volume seen with the branched TMED, with both molecules occupying similar volumes yet with a more pronounced role for the different types of amine functional groups on the change in the density and primary groups having larger densities than tertiary groups, due to the additional hydrogen atoms. Further reduction in molecular volume, and subsequently, increase in density, is seen with cyclic amines such as DMPZ and HEP and branched structures such as the DEEA. Another observation concerns the type of functional groups seen with 2BAE with its secondary amine and hydroxyl end group, with its lower volume compared to HDMA with its two primary end groups, with the strong interactions between the NH–OH groups being more effective in allowing the chain to coil on itself.

From a technical perspective, solvents with lower densities on account of their large molecule volumes tend to increase the unit cost of the capture plant due to the larger sizing of the processing units.⁸⁵ Hence, it is preferred to design solvents with larger densities that can be obtained by reducing the volume occupied by the molecule. This can be done by having short-chain molecules, with either branched or cyclic structures and the presence of strong functional groups such as primary amines and hydroxyl groups exploiting intramolecular interactions that can allow the molecule to compact its volume.

The same approach has also been applied to viscosity, heat capacity, and heat of vaporization, shown in *Figure 7*, predicted from soft-SAFT at 313 K, explicitly showing members with three to six carbons from linear monoamine primary aminoalcohols and secondary alkyl ethanolamines and for linear diamines diamino alkanes.

Considering that viscosity is a volumetric property, as with density, it was also correlated with the molecular volume, as shown in *Figure 7(a)*. Opposite to density, short-chain molecules with small molecular volumes tend to have smaller viscosities due to reduced friction between the smaller molecules. This trend is also seen in other amine families such as aminoalcohols and diamines. Interestingly, the ranking of the viscosity is in the order of aminoalcohols > alkyl ethanolamines > diamino alkanes. For molecules with the same

carbon number, three carbons, the viscosity is in the order of 3A1P > 2MAE > 1,3 DiAP, which might be related to the effect of the functional groups on the strength of interactions with other molecules and their relations to increasing the friction between molecules. For example, the presence of the hydroxyl group in 3A1P, compared to the primary amine end group in 1,3 DiAP, contributed to stronger associations with other molecules, hence, larger friction and viscosity. Also, for 3A1P and 2MAE, the difference is the secondary amine group with its weaker association in the latter compared to the presence of primary amine in the former.

Viscosity impacts the hold-up of the amine in the absorber, and the mass transfer of the gas in the liquid phase is hindered at higher viscosities.⁸⁵ Longer contact times are required for the same degree of separation, resulting in larger absorption towers and increased total cost. As such, low-viscosity amines are preferred, which are found with short-chain molecules to reduce friction with other molecules, and those with weaker functional groups such as tertiary amines to reduce the tendency to associate with other molecules and form clusters.

In the same direction, vapor pressure, heat capacity, and heat of vaporization are correlated with molecular energy as they are energetic properties reliant on the strength of intermolecular interactions in the molecule. From *Figure 7(b–d)*, increasing the energy of the entire molecule increases the magnitude of these properties, except vapor pressure. For vapor pressure, larger molecules tend to have lower vapor pressure values due to the stronger dispersive interactions, reducing the tendency of the molecules to escape from the liquid to the vapor phase, as seen with an increasing chain length of the alkyl ethanolamines, moving from the three-carbon 2MAE to the six-carbon 2BAE in *Figure 7(b)*. Across families, the change in vapor pressure is in the order of aminoalcohols < alkyl ethanolamines < diamino alkanes because of the impact of functional groups on the strength of association interactions. This is seen with stronger NH₂–OH in aminoalcohols interactions compared to either NH–OH in alkyl ethanolamines or NH₂–NH₂ interactions in diamines. These interactions are also responsible for the increasing trends in heat of vaporization for these molecules, which is opposite to the vapor pressure (see *Figure 7(c)*). Larger molecules and those with functionalities indicative of stronger interactions tend to require larger amounts of energy to induce a phase change.

In terms of heat capacity, the same general trend is also observed in *Figure 7(d)*, with larger molecules in the same family having larger heat capacities linearly correlated with the molecular energy. Moving across families, the ranking is different than that seen with the heat of vaporization, following the order of alkyl ethanolamines > diamino alkanes > aminoalcohols due to the equally impacting role played by molecular volume, as larger molecules have larger capacities to absorb heat in the liquid state.

The heat capacity and heat of vaporization are components of the regeneration energy, which is 70% of the total energy cost, used as a performance indicator for carbon capture.⁸⁶ Hence, it is imperative to choose amine molecules with a lower heat capacity and heat of vaporization to reduce the reboiler duty while also having reduced vapor pressure to limit solvent losses and reduce associated operational costs. While smaller molecules with weaker functionalities tend to have lower heat capacity and heat of vaporization, their vapor pressure tends to be high. Hence, branching or formation of cyclic structures might be an intermediate solution, as the steric hindrance

might reduce the formation of association interactions conducive to the high heat of vaporization, coupled with their compacted volumes resulting in low heat capacities. This is seen in the case of cyclic monoamine and diamines with at least 30% lower heat of vaporization and 60% lower heat capacity compared to linear monoamine and diamines, still with almost 3-fold vapor pressure.^{87–89}

In addition to the use of soft-SAFT for the properties already presented, COSMO-RS was used as an additional molecular modeling tool to determine the pK_a values of the pure alternative amines. pK_a provides the amine basicity, with higher values indicative of a stronger base. Accordingly, the amine molecule can easily be deprotonated, increasing its CO_2 absorption capacity, which is one of the critical properties of novel solvents for CO_2 capture. Provided in Figure 8, are the

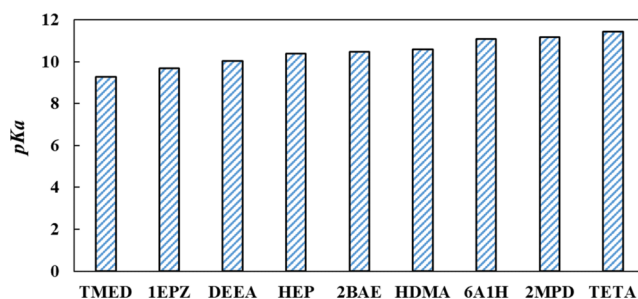


Figure 8. COSMO-RS predicted pK_a values of selected alternative amines with six-carbon atoms.

COSMO-RS predicted pK_a values for amines with six-carbon atoms with a variety of structures, including primary (6A1H), secondary (2BAE), tertiary (DEEA), cyclic (1EPZ, HEP, 2MPD), diamine (HDMA, TMED), and polyamine (TETA).

The largest pK_a value was obtained for TETA at a value of 11.4, owing to the presence of two pairs of primary and secondary amine groups in its structure, while the least was obtained from TMED at a value of 9.3, due to the presence of two tertiary amine group. These results are consistent with Vijisha et al.,²⁹ who calculated the pK_a values of these amines using DFT. It was determined that two factors affect the pK_a values including the lone electron pairs and hydrogen bonding, with more lone pairs on the amine and hydrogen bonding indicating larger pK_a values. This justifies the low value for TMED with its sterically hindered structure reducing its

tendency to form hydrogen bonding and the presence of tertiary amine groups with a low number of lone electron pairs.

Figure 8 depicts results on alternative amines with linear carbon chains and one amine functional group, including DEEA, 2BAE, and 6A1H. The order of increasing pK_a , and hence CO_2 affinity, is DEEA < 2BAE < 6A1H, moving from the tertiary amine group to primary amine, in accordance with results given in the literature and the tendency of the amine groups to form hydrogen bonding.²⁹ Another factor to consider is the number and the type of functional groups in the structure. For example, TMED has two tertiary amines, with its counterpart being DEEA with one tertiary amine and a hydroxyl group. The same can be observed for HDMA with two primary amine end groups and its counterpart 6A1H with one primary amine and one hydroxyl end group. Notice that for these amines the pK_a values are TEMD < DEEA, and HDMA < 6A1H, indicating that the presence of the hydroxyl group can further increase the deprotonation rate of the amine molecule and formation of free ions in the solution and increase its affinity toward CO_2 , being more effective than having an additional amine group in place of the hydroxyl group. The same observation is seen for the cyclic 1EPZ with a secondary and tertiary amine group and its counterpart HEP with an additional hydroxyl group.

Lastly, the geometric structure of the molecule also plays a role, with 6A1H possessing a primary amine group and a hydroxyl group and its pK_a value being lower than the cyclic 2MPD with a secondary amine group, due to the reduced molecular volume of the latter, facilitating the formation of hydrogen bonding, as hydrogen bonding is more critical for the pK_a value of cyclic molecules.

4.4. Ranking of Promising Alternative Amines Using Statistical Analysis Tools. From the preceding section, a trade-off emerged on the influence of molecular features on properties, for CO_2 capture, with the molecular structure in terms of carbon chain length and branching being more important for volumetric and thermal properties, while the degree of functionalization has a higher impact on the CO_2 affinity. Considering these trade-offs, GRA and TOPSIS were used to rank the promising amines based on the criteria in Table 1. These properties were obtained from soft-SAFT and COSMO-RS at $T = 313$ K, representative of typical CO_2 capture conditions, and assigned different weights to reduce them into a single-objective function based on the procedure for GRA and TOPSIS.

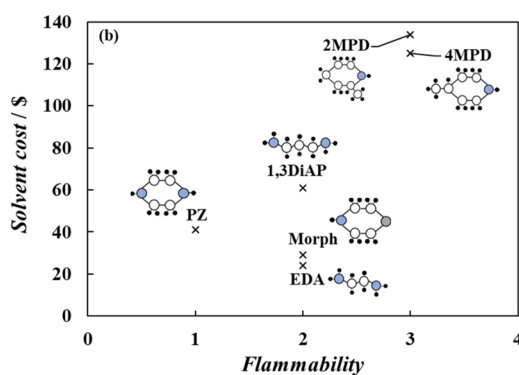


Figure 9. (a) Ranking of top ten amine molecules using GRA and TOPSIS methods and (b) cost and flammability (based on flash point) of best-performing amine molecules common to GRA, TOPSIS, and manual sorting, with (x) marking the position of the amine.

The results for the ranking of the best ten performing amine molecules are included in Figure 9, based on GRA and TOPSIS results included in Table S4 in the SI. It should be noted that the results of this analysis are simplistic based on the assumptions included in this work and should be treated with care when expanding to other conditions.

Although GRA and TOPSIS are inherently different, they presented the same eight amine molecules in the ranking list including EDA and 1,3 DiAP, PZ, Morph, 2MPD, 2MPD, 4MPD, M-4PDiol, and 2MAE. From the GRA method, MEA was found to be the most promising solvent, followed by EDA, while the TOPSIS method established PZ as the most promising solvent, also followed by EDA. Notice that for both methods, cyclic molecules are among the top five most promising solvents. In order to ensure the absence of bias from the statistical method, a simplistic manual sorting of the studied amines with the same objective for the studied properties showed that the most promising amines common among all methods are indeed the cyclic 2MPD, 4MPD, Morph, and PZ, and linear EDA and 1,3DiAP. To this set of promising amines, their flammability and cost have been included as additional criteria, shown in Figure 9. The flammability values for the amines are taken from the Santa Cruz Biotechnology material safety data sheets (MSDS) database.⁹⁰ The numerical values represent the flash points for each amine ranging from 0 to 4, from nonflammable to highly flammable, while the cost of the amine in USD\$ per 500 mL was obtained from literature sources,⁹¹ preferring solvents with low flammability and cost. Both 2MPD and 4MPD have high flammability and cost, which rule them out as potential solvents. Alternatively, PZ has the lowest flammability compared to Morph and EDA, yet at twice the cost.

Accordingly, it can be concluded that the most promising alternative amines for next-generation carbon capture absorption plants, aside from the well-studied PZ, are the diamine EDA and the cyclic Morph Villarroel et al.,⁹² analyzed EDA as a solvent, showing its higher CO₂ absorption capacity and lower corrosivity compared to MEA and DEA. Mazari et al.,⁹³ investigated the impact of Morph on CO₂ solubility, demonstrating better reactivity than MEA and a higher CO₂ absorption rate. The potential of these solvents at large scale, including capture performance, regeneration requirements, long-term stability, and others, is an area for future work. These results demonstrate the potential of applying molecular modeling tools for a systematic screening, allowing the prioritization of promising alternative solvents for CO₂ capture with reduced time and cost requirements, granting the use of physically grounded models such as soft-SAFT EoS.

5. CONCLUSIONS

CO₂ emissions have become the chief driver for the current climate change and global warming phenomena, with CO₂ capture using absorption identified as the most mature technology available and readily deployable to the market. Nevertheless, high solvent regeneration energy and low stability are bottlenecks impeding the rapid penetration of this technology at a low capture cost. In this work, 37 amine molecules with different structures and functionalities have been examined as alternative solvents for CO₂ capture, employing a molecular-based EoS, soft-SAFT, complemented with quantum chemical calculations using COSMO-RS and statistical analysis tools. Coarse-grain molecular models have been proposed capturing key structural and energetic features

of the pure alternative amines, and the models have been characterized using available experimental data to ensure high fidelity in them. This was followed by the predictions of fundamental thermodynamic properties of interest for CO₂ capture including density, vapor pressure, heat capacity, enthalpy of vaporization, viscosity, and pK_a.

Key molecular insights into the effect of molecular structure and functional groups on the observed properties were drawn. It has been established that carbon chain length, followed by the geometric structure (i.e., linear, branched, and cyclic), and the last number and the type of functionalization have a direct impact on density, viscosity, vapor pressure, heat capacity, and heat of vaporization, with short-chain molecules being preferred to ensure optimal performance across these properties. Alternatively, high affinity for the solvents for CO₂ requires a high degree of functionalization mainly with the addition of either primary or secondary amine groups along with the presence of hydroxyl groups.

The trade-offs between these properties were captured using a multidecision criteria approach employing statistical tools such as GRA and TOPSIS, to reduce these properties into a single-objective function. This narrowed down the best six performing solvents to be the cyclic 2MPD, 4MPD, Morph, PZ, diamine EDA, and 1,3DiAP, with a fine balance between their properties of interest, with particular interest in EDA and Morph as promising next-generation solvents.

This work demonstrates the capabilities of molecular modeling tools in providing a reliable platform for modeling, screening, and selecting promising solvents for CO₂ capture. Additionally, the core strength of these tools has been established by providing a direct link between microlevel molecular features and macro-level behavior, guiding future solvent design and synthesis. The molecular-level insights with tools such as the ones used in this work should be used as the basis for the future design of molecules with attractive properties for CO₂ capture including affinity to CO₂, low regeneration energy requirements, and excellent transport properties. Additional examination of the role of the molecular-level precursors on the solvent long-term stability and performance at scale, followed by a techno-economic and environmental assessment, is also key for future research and large-scale implementation.

■ ASSOCIATED CONTENT

SI Supporting Information

The Supporting Information is available free of charge at <https://pubs.acs.org/doi/10.1021/acs.energyfuels.4c03210>.

Experimental data, association sites, and correlations for molecular parameters, predicted density, vapor pressure, heat capacity, and heat of vaporization from soft-SAFT compared to experimental data ([PDF](#))

■ AUTHOR INFORMATION

Corresponding Author

Lourdes F. Vega — Research and Innovation Centre on CO₂ and Hydrogen (RICH Center) and Chemical and Petroleum Engineering Department, Khalifa University of Science and Technology, 127788 Abu Dhabi, United Arab Emirates;
ORCID: [0000-0002-7609-4184](https://orcid.org/0000-0002-7609-4184); Email: lourdes.vega@ku.ac.ae

Authors

Fareeha Shadab – Research and Innovation Centre on CO₂ and Hydrogen (RICH Center) and Chemical and Petroleum Engineering Department, Khalifa University of Science and Technology, 127788 Abu Dhabi, United Arab Emirates
Ismail I. I. Alkhatib – Research and Innovation Centre on CO₂ and Hydrogen (RICH Center) and Chemical and Petroleum Engineering Department, Khalifa University of Science and Technology, 127788 Abu Dhabi, United Arab Emirates; [@orcid.org/0000-0002-6769-5383](https://orcid.org/0000-0002-6769-5383)

Complete contact information is available at:
<https://pubs.acs.org/10.1021/acs.energyfuels.4c03210>

Author Contributions

F.S.: Data curation, investigation, writing, original draft, and formal analysis. I.I.I.A.: Conceptualization, methodology, software, reviewing, and editing. L.F.V.: Conceptualization, resources, software, supervision, writing, review and editing, and funding acquisition.

Notes

The authors declare no competing financial interest.

ACKNOWLEDGMENTS

This work was funded by the Khalifa University of Science and Technology under project RC2–2019–007 to the Research and Innovation Center in CO₂ and Hydrogen (RICH Center). Computational resources from the RICH Center and the KU Research Computing Department are gratefully acknowledged.

NOMENCLATURE

1A2P	1-amino-2-propanol
1M-2PPE	1-methyl-2-piperidineethanol
1EPZ	1-ethyl piperazine
1MPZ	1-methyl piperazine
1,3 DiAP	1,3-diaminopropane
2BAE	2-(butylamino)ethanol
2MAE	2-(methylamino)ethanol
2MPD	2-methylpiperidine
3A1P	3-amino-1-propanol
4-AMTHP	4-aminomethyltetrahydropyran
4MPD	4-methylpiperidine
5A1P	5-amino-1-pentanol
6A1H	6-amino-1-hexanol
AAD	average absolute deviation
AAEA	2-(2-aminoethylamino)ethanol
B	free-volume overlap among the molecules
CCUS	carbon capture, utilization, and storage
COSMO-RS	conductor-like screening model for real solvents
CPA	cubic-plus association
C _p	isobaric heat capacity
DEEA	2-(diethylamino)ethanol
DETA	diethylene-triamine
DFT	density functional theory
DMPZ	1,4-dimethylpiperazine
EDA	ethylenediamine
EoS	equation of state
FVT	free-volume theory
GC	coarse-grained model
GRA	gray relational analysis
ΔH ^{ap}	heat of vaporization
HDMA	hexamethylenediamine
HEP	N-(2-hydroxyethyl)piperazine

IBAE	2-(isobutylamino)ethanol
IPAE	2-(isopropylamino)ethanol
IPDEA	2-(isopropyl)diethanolamine
L _v	length parameter of the molecule's structure
LFER	linear free energy relationship
LJ	Lennard-Jones
m	chain length
MAPA	N-methyl-1,3-propanediamine
MEA	monoethanolamine
Morph	morpholine
M _w	molecular weight
PCC	postcombustion capture
PMDETA	pentamethyl-divinyl-triamine
PZ	piperazine
SAFT	statistical associating fluid theory
TETA	triethylenetetramine
TMED	1,2-bis(dimethylamino)ethane
TOPSIS	technique for order of preference by similarity to ideal solution
TPT1	1st order thermodynamic perturbation theory
VLE	vapor–liquid equilibria
x _p	fraction of polar segment

GREEK SYMBOLS

α	proportionality between the energy barrier and the density
ϵ_i/k_B	dispersive energy (K)
ϵ^{HB}	association energy (K)
<i>me</i>	energy of molecule
$m\sigma^3$	volume of molecule
η_{ij}	adjustable size binary parameter
η	viscosity
κ^{HB}	association volume (\AA^3)
μ	experimental dipole moment ($\text{C}\cdot\text{m}^2$)
ξ_{ij}	adjustable energy binary parameter
σ_i	segment diameter (\AA)

REFERENCES

- (1) Lüthi, D.; Le Floch, M.; Bereiter, B.; Blunier, T.; Barnola, J. M.; Siegenthaler, U.; Raynaud, D.; Jouzel, J.; Fischer, H.; Kawamura, K.; Stocker, T. F. High-Resolution Carbon Dioxide Concentration Record 650,000–800,000 Years before Present. *Nature* **2008**, *453* (7193), 379–382.
- (2) Algayerova, O.; Bárcena, A.; Dashti, R.; Alishahbana, A. S.; Songwe, V. UNSDG—Scaling Carbon Dioxide Removal to Achieve Climate Targets, 2021. <https://unsgd.un.org/latest/blog/scaling-carbon-dioxide-removal-achieve-climate-targets>.
- (3) Song, C.; Liu, Q.; Deng, S.; Li, H.; Kitamura, Y. Cryogenic-Based CO₂ Capture Technologies: State-of-the-Art Developments and Current Challenges. *Renewable Sustainable Energy Rev.* **2019**, *101*, 265–278, DOI: [10.1016/J.RSER.2018.11.018](https://doi.org/10.1016/J.RSER.2018.11.018).
- (4) Report: *State of the Art: CCS Technologies* 2023; Global CCS Institute, 2023.
- (5) Report: *Carbon Capture in 2021: Off and Running or Another False Start?*; International Energy Agency: 2021.
- (6) Koitsoumpa, E. I.; Bergins, C.; Kakaras, E. The CO₂ Economy: Review of CO₂ Capture and Reuse Technologies. *J. Supercrit. Fluids* **2018**, *132*, 3–16.
- (7) Odunlami, O. A.; Vershma, D. A.; Oladimeji, T. E.; Nkongho, S.; Ogunlade, S. K.; Fakinle, B. S. Advanced Techniques for the Capturing and Separation of CO₂ – A Review. *Results Eng.* **2022**, *15*, No. 100512.
- (8) Meng, F.; Meng, Y.; Ju, T.; Han, S.; Lin, L.; Jiang, J. Research Progress of Aqueous Amine Solution for CO₂ Capture: A Review. *Renewable Sustainable Energy Rev.* **2022**, *168*, No. 112902.

- (9) Yamada, H. Amine-Based Capture of CO₂ for Utilization and Storage. *Polym. J.* **2021**, 53 (1), 93–102.
- (10) Mumford, K. A.; Wu, Y.; Smith, K. H.; Stevens, G. W. Review of Solvent Based Carbon-Dioxide Capture Technologies. *Front. Chem. Sci. Eng.* **2015**, 9 (2), 125–141.
- (11) Khalifa, O.; Alkhatib, I. I. I.; Bahamon, D.; Alhajaj, A.; Abu-Zahra, M. R. M.; Vega, L. F. Modifying Absorption Process Configurations to Improve Their Performance for Post-Combustion CO₂ Capture—What Have We Learned and What Is Still Missing? *Chem. Eng. J.* **2022**, 430, No. 133096.
- (12) Campbell, Z. S.; Han, S.; Marre, S.; Abolhasani, M. Continuous Flow Solar Desorption of CO₂ from Aqueous Amines. *ACS Sustainable Chem. Eng.* **2021**, 9 (6), 2570–2579.
- (13) Barpaga, D.; Jiang, Y.; Zheng, R. F.; Malhotra, D.; Koech, P. K.; Zwoster, A.; Mathias, P. M.; Hedebrant, D. J. Evaluation of a Third Generation Single-Component Water-Lean Diamine Solvent for Post-Combustion CO₂ Capture. *ACS Sustainable Chem. Eng.* **2022**, 10 (14), 4522–4528.
- (14) Ye, J.; Jiang, C.; Chen, H.; Shen, Y.; Zhang, S.; Wang, L.; Chen, J. Novel Biphasic Solvent with Tunable Phase Separation for CO₂ Capture: Role of Water Content in Mechanism, Kinetics, and Energy Penalty. *Environ. Sci. Technol.* **2019**, 53 (8), 4470–4479.
- (15) Hedebrant, D. J.; Koech, P. K.; Glezakou, V. A.; Rousseau, R.; Malhotra, D.; Cantu, D. C. Water-Lean Solvents for Post-Combustion CO₂ Capture: Fundamentals, Uncertainties, Opportunities, and Outlook. *Chem. Rev.* **2017**, 117 (14), 9594–9624.
- (16) Liu, A. H.; Zheng, Y. J.; Ma, G. T.; Shi, D. N.; Ren, B. H.; Lu, X. B. Dual-Functionalized Amines as Single-Component Water-Lean CO₂ Absorbents with Low-Viscosity and High-Capacity: The Synergistic Effect of Alkoxy and Silyl Groups. *Sep. Purif. Technol.* **2024**, 333, No. 125922.
- (17) Ping, T.; Dong, Y.; Shen, S. Energy-Efficient CO₂ Capture Using Nonaqueous Absorbents of Secondary Alkanolamines with a 2-Butoxyethanol Cosolvent. *ACS Sustainable Chem. Eng.* **2020**, 8 (49), 18071–18082.
- (18) Karlsson, H. K.; Makhool, H.; Karlsson, M.; Svensson, H. Chemical Absorption of Carbon Dioxide in Non-Aqueous Systems Using the Amine 2-Amino-2-Methyl-1-Propanol in Dimethyl Sulfoxide and N-Methyl-2-Pyrrolidone. *Sep. Purif. Technol.* **2021**, 256, No. 117789.
- (19) Hedayati, A.; Feyzi, F. CO₂ -Binding Organic Liquids Comprised of 1,1,3,3-Tetramethylguanidine and Alkanol for Post-combustion CO₂ Capture: Water Inhibitory Effect of Amine Promoters. *ACS Sustainable Chem. Eng.* **2020**, 8 (21), 7909–7920.
- (20) Gautam, A.; Mondal, M. K. Review of Recent Trends and Various Techniques for CO₂ Capture: Special Emphasis on Biphasic Amine Solvents. *Fuel* **2023**, 334, No. 126616.
- (21) Bui, T. Q.; Khokarale, S. G.; Shukla, S. K.; Mikkola, J. P. Switchable Aqueous Pentaethylenehexamine System for CO₂ Capture: An Alternative Technology with Industrial Potential. *ACS Sustainable Chem. Eng.* **2018**, 6 (8), 10395–10407.
- (22) Song, T.; Chen, W.; Zhang, Y.; Situ, G.; Liu, F.; Shen, Y.; Kong, W.; Zhong, X.; Huang, Y.; Li, S.; Yang, L.; Zhang, S.; Li, S.; Li, W. Mass Transfer and Reaction Mechanism of CO₂ Capture into a Novel Amino Acid Ionic Liquid Phase-Change Absorbent. *Sep. Purif. Technol.* **2024**, 330, No. 125538.
- (23) Eichenlaub, J.; Baran, K.; Smiechowski, M.; Kłoskowski, A. Free Volume in Physical Absorption of Carbon Dioxide in Ionic Liquids: Molecular Dynamics Supported Modeling. *Sep. Purif. Technol.* **2023**, 313, No. 123464.
- (24) Soo, X. Y. D.; Lee, J. J. C.; Wu, W. Y.; Tao, L.; Wang, C.; Zhu, Q.; Bu, J. Advancements in CO₂ Capture by Absorption and Adsorption: A Comprehensive Review. *J. CO₂ Util.* **2024**, 81, No. 102727.
- (25) Hanifa, M.; Agarwal, R.; Sharma, U.; Thapliyal, P. C.; Singh, L. P. A Review on CO₂ Capture and Sequestration in the Construction Industry: Emerging Approaches and Commercialised Technologies. *J. CO₂ Util.* **2023**, 67, No. 102292.
- (26) Borhani, T. N.; Wang, M. Role of Solvents in CO₂ Capture Processes: The Review of Selection and Design Methods. *Renewable Sustainable Energy Rev.* **2019**, 114, No. 109299.
- (27) Wang, B.; Chen, J.; Wang, J.; Xu, Z.; Zhao, W. Molecular Insights into the Absorption of SO₂ with Amine Alkyl Organosilicon and Its Optimal Absorption Temperature. *Sep. Purif. Technol.* **2024**, 340, No. 126660.
- (28) Wang, K.; Li, G.; Li, Y.; Chen, Y.; Zhang, L.; Zhu, Z.; Xu, Z.; Zhao, W. Entropy Enthalpy Compensation in the SO₂ Absorption Reaction and the Optimal Capture Temperature Range with Amine Alkyl Siloxane as Absorbent. *Sep. Purif. Technol.* **2023**, 306, No. 122581.
- (29) Vijisha, K. R.; Muraleedharan, K. The PK_a Values of Amine Based Solvents for CO₂ Capture and Its Temperature Dependence—An Analysis by Density Functional Theory. *Int. J. Greenhouse Gas Control* **2017**, 58, 62–70.
- (30) Chowdhury, F. A.; Yamada, H.; Matsuzaki, Y.; Goto, K.; Higashii, T.; Onoda, M. Development of Novel Synthetic Amine Absorbents for CO₂ Capture. *Energy Procedia* **2014**, 63, 572–579.
- (31) Singh, P.; Niederer, J. P. M.; Versteeg, G. F. Structure and Activity Relationships for Amine Based CO₂ Absorbents-I. *Int. J. Greenhouse Gas Control* **2007**, 1 (1), 5–10.
- (32) Singh, P.; Niederer, J. P. M.; Versteeg, G. F. Structure and Activity Relationships for Amine-Based CO₂ Absorbents-II. *Chem. Eng. Res. Des.* **2009**, 87 (2), 135–144.
- (33) Conway, W.; Yang, Q.; James, S.; Wei, C. C.; Bown, M.; Feron, P.; Puxty, G. Designer Amines for Post Combustion CO₂ Capture Processes. *Energy Procedia* **2014**, 63, 1827–1834.
- (34) Li, L.; Clifford, S.; Puxty, G.; Maeder, M.; Burns, R.; Yu, H.; Conway, W. Kinetic and Equilibrium Reactions of a New Heterocyclic Aqueous 4-Aminomethyltetrahydropyran (4-AMTHP) Absorbent for Post Combustion Carbon Dioxide (CO₂) Capture Processes. *ACS Sustainable Chem. Eng.* **2017**, 5 (10), 9200–9206.
- (35) Madejski, P.; Chmiel, K.; Subramanian, N.; Kus, T. Methods and Techniques for CO₂ Capture: Review of Potential. *Energies* **2022**, 15, No. 887.
- (36) Vega, F.; Baena-Moreno, F. M.; Gallego Fernández, L. M.; Portillo, E.; Navarrete, B.; Zhang, Z. Current Status of CO₂ Chemical Absorption Research Applied to CCS: Towards Full Deployment at Industrial Scale. *Appl. Energy* **2020**, 260, No. 114313.
- (37) Wang, R.; Zhao, H.; Qi, C.; Yang, X.; Zhang, S.; Li, M.; Wang, L. Novel Tertiary Amine-Based Biphasic Solvent for Energy-Efficient CO₂ Capture with Low Corrosivity. *Energy* **2022**, 260, No. 125045.
- (38) Dziejarski, B.; Serafin, J.; Andersson, K.; Krzyżyska, R. CO₂ Capture Materials: A Review of Current Trends and Future Challenges. *Mater. Today Sustainability* **2023**, 24, No. 100483.
- (39) Zhang, R.; Liu, R.; Barzaghi, F.; Sanku, M. G.; Li, C.; Xiao, M. CO₂ Absorption in Blended Amine Solvent: Speciation, Equilibrium Solubility and Excessive Property. *Chem. Eng. J.* **2023**, 466, No. 143279.
- (40) Zhang, R.; Li, Y.; He, X.; Niu, Y.; Li, C.; Amer, M. W.; Barzaghi, F. Investigation of the Improvement of the CO₂ Capture Performance of Aqueous Amine Sorbents by Switching from Dual-Amine to Trio-Amine Systems. *Sep. Purif. Technol.* **2023**, 316, No. 123810.
- (41) Liang, Z.; Fu, K.; Idem, R.; Tontiwachwuthikul, P. Review on Current Advances, Future Challenges and Consideration Issues for Post-Combustion CO₂ Capture Using Amine-Based Absorbents. *Chin. J. Chem. Eng.* **2016**, 24 (2), 278–288.
- (42) Dutcher, B.; Fan, M.; Russell, A. G. Amine-Based CO₂ Capture Technology Development from the Beginning of 2013—A Review. *ACS Appl. Mater. Interfaces* **2015**, 7 (4), 2137–2148.
- (43) Aghel, B.; Janati, S.; Wongwises, S.; Shadloo, M. S. Review on CO₂ Capture by Blended Amine Solutions. *Int. J. Greenhouse Gas Control* **2022**, 119, No. 103715.
- (44) Perdomo, F. A.; Khalit, S. H.; Graham, E. J.; Tzirakis, F.; Papadopoulos, A. I.; Tsivintzelis, I.; Seferlis, P.; Adjiman, C. S.; et al. A Predictive Group-Contribution Framework for the Thermodynamic Modelling of CO₂ Absorption in Cyclic Amines, Alkyl Polyamines,

- Alkanolamines and Phase-Change Amines: New Data and SAFT- γ Mie Parameters. *Fluid Phase Equilib.* **2023**, *566*, No. 113635.
- (45) Dowell, N. M.; Llovel, F.; Adjiman, C. S.; Jackson, G.; Galindo, A. Modeling the Fluid Phase Behavior of Carbon Dioxide in Aqueous Solutions of Monoethanolamine Using Transferable Parameters with the SAFT-VR Approach. *Ind. Eng. Chem. Res.* **2010**, *49* (4), 1883–1899.
- (46) Rodriguez, J.; Dowell, N. M.; Llovel, F.; Adjiman, C. S.; Jackson, G.; Galindo, A. Modelling the Fluid Phase Behaviour of Aqueous Mixtures of Multifunctional Alkanolamines and Carbon Dioxide Using Transferable Parameters with the SAFT- VR Approach. *Mol. Phys.* **2012**, *110* (11–12), 1325–1348.
- (47) Chremos, A.; Forte, E.; Papaioannou, V.; Galindo, A.; Jackson, G.; Adjiman, C. S. Modelling the Phase and Chemical Equilibria of Aqueous Solutions of Alkanolamines and Carbon Dioxide Using the SAFT- γ SW Group Contribution Approach. *Fluid Phase Equilib.* **2016**, *407*, 280–297.
- (48) Nguyenhuynh, D.; Nguyen-thi, T. Modeling the Fluid Phase Behavior of Amines, Aromatic Amines and Their Mixtures Using the Modified Group-Contribution PC-SAFT. *Fluid Phase Equilib.* **2022**, *551*, No. 113274.
- (49) Wang, T.; El Ahmar, E.; Coquelet, C.; Kontogeorgis, G. M. Improvement of the PR-CPA Equation of State for Modelling of Acid Gases Solubilities in Aqueous Alkanolamine Solutions. *Fluid Phase Equilib.* **2018**, *471*, 74–87.
- (50) Wang, T.; Guittard, P.; Coquelet, C.; El Ahmar, E.; Baudouin, O.; Kontogeorgis, G. M. Corrigendum to “Improvement of the PR-CPA Equation of State for Modelling of Acid Gases Solubilities in Aqueous Alkanolamine Solutions. *Fluid Phase Equilib.* **2019**, *485*, 126–127.
- (51) Blas, F. J.; Vega, L. F. Thermodynamic Behaviour of Homonuclear and Heteronuclear Lennard-Jones Chains with Association Sites from Simulation and Theory. *Mol. Phys.* **1997**, *92* (1), 135–150.
- (52) Lloret, J. O.; Vega, L. F.; Llovel, F. A Consistent and Transferable Thermodynamic Model to Accurately Describe CO₂ Capture with Monoethanolamine. *J. CO₂ Util.* **2017**, *21*, 521–533.
- (53) Pereira, L. M. C.; Vega, L. F. A Systematic Approach for the Thermodynamic Modelling of CO₂-Amine Absorption Process Using Molecular-Based Models. *Appl. Energy* **2018**, *232*, 273–291.
- (54) Alkhatib, I. I. I.; Pereira, L. M. C.; Alhajaj, A.; Vega, L. F. Performance of Non-Aqueous Amine Hybrid Solvents Mixtures for CO₂ Capture: A Study Using a Molecular-Based Model. *J. CO₂ Util.* **2020**, *35*, 126–144.
- (55) Bahamon, D.; Alkhatib, I. I. I.; Alkhatib, N.; Builes, S.; Sinnokrot, M.; Vega, L. F. A Comparative Assessment of Emerging Solvents and Adsorbents for Mitigating CO₂ Emissions from the Industrial Sector by Using Molecular Modeling Tools. *Front. Energy Res.* **2020**, *8*, No. 165.
- (56) Pereira, L. M. C.; Llovel, F.; Vega, L. F. Thermodynamic Characterisation of Aqueous Alkanolamine and Amine Solutions for Acid Gas Processing by Transferable Molecular Models. *Appl. Energy* **2018**, *222*, 687–703.
- (57) de Salazar Martínez, E. M.; Alexandre-Franco, M. F.; Nieto-Sánchez, A. J.; Cuerda-Correa, E. M. Exploring the Role of Surface and Porosity in CO₂ Capture by CaO-Based Adsorbents through Response Surface Methodology (RSM) and Artificial Neural Networks (ANN). *J. CO₂ Util.* **2024**, *83*, No. 102773.
- (58) Madeira, L.; Teixeira, M. R.; Carvalho, F. Modeling and Optimization of Atmospheric CO₂ Capture for Neutralization of High Alkaline Wastewaters Using Response Surface Methodology. *J. CO₂ Util.* **2024**, *81*, No. 102705.
- (59) Balaraman, H. B.; Rangarajan, V.; Rathnasamy, S. K. A Synergetic Green Approach for Enhanced CO₂ capture in Protic Deep Eutectic Mixtures - Kinetics and Henry's Solubility Determination. *J. CO₂ Util.* **2022**, *65*, No. 102217.
- (60) Hamzehie, M. E.; Najibi, H. Experimental and Theoretical Study of Carbon Dioxide Solubility in Aqueous Solution of Potassium Glycinate Blended with Piperazine as New Adsorbents. *J. CO₂ Util.* **2016**, *16*, 64–77.
- (61) Sedghamiz, M. A.; Rasoolzadeh, A.; Rahimpour, M. R. The Ability of Artificial Neural Network in Prediction of the Acid Gases Solubility in Different Ionic Liquids. *J. CO₂ Util.* **2015**, *9*, 39–47.
- (62) Alkhatib, I. I. I.; Kahlika, O.; Bahamon, D.; Abu-Zahra, M. R. M.; Vega, L. F. Sustainability Criteria as a Game Changer in the Search for Hybrid Solvents for CO₂ and H₂S Removal. *Sep. Purif. Technol.* **2021**, *277*, No. 119516.
- (63) Johnson, J. K.; Zollwef, J. A.; Gubbins, K. E. The Lennard-Jones Equation of State Revisited. *Mol. Phys.* **1993**, *78* (3), 591–618.
- (64) Chapman, W. G.; Gubbins, K. E.; Jackson, G.; Radosz, M. SAFT: Equation-of-State Solution Model for Associating Fluids. *Fluid Phase Equilib.* **1989**, *52*, 31–38.
- (65) Chapman, W. G.; Gubbins, K. E.; Jackson, G.; Radosz, M. New Reference Equation of State for Associating Liquids. *Ind. Eng. Chem. Res.* **1990**, *29* (8), 1709–1721.
- (66) Wertheim, M. S. Fluids with Highly Directional Attractive Forces. IV. Equilibrium Polymerization. *J. Stat. Phys.* **1986**, *42* (3–4), 477–492.
- (67) Wertheim, M. S. Fluids with Highly Directional Attractive Forces. III. Multiple Attraction Sites. *J. Stat. Phys.* **1986**, *42* (3–4), 459–476.
- (68) Wertheim, M. S. Fluids with Highly Directional Attractive Forces. II. Thermodynamic Perturbation Theory and Integral Equations. *J. Stat. Phys.* **1984**, *35* (1–2), 35–47.
- (69) Wertheim, M. S. Fluids with Highly Directional Attractive Forces. I. Statistical Thermodynamics. *J. Stat. Phys.* **1984**, *35* (1–2), 19–34.
- (70) Gubbins, K. E.; Twu, C. H. Thermodynamics of Polyatomic Fluid Mixtures-I: Theory. *Chem. Eng. Sci.* **1978**, *33* (7), 863–878.
- (71) Twu, C. H.; Gubbins, K. E. Thermodynamics of Polyatomic Fluid Mixtures—II: Polar, Quadrupolar and Octopolar Molecules. *Chem. Eng. Sci.* **1978**, *33* (7), 879–887.
- (72) Jog, P. K.; Chapman, W. G. Application of Wertheim's Thermodynamic Perturbation Theory to Dipolar Hard Sphere Chains. *Mol. Phys.* **1999**, *97* (3), 307–319.
- (73) Jog, P. K.; Sauer, S. G.; Blaesing, J.; Chapman, W. G. Application of Dipolar Chain Theory to the Phase Behavior of Polar Fluids and Mixtures. *Ind. Eng. Chem. Res.* **2001**, *40* (21), 4641–4648.
- (74) Alkhatib, I. I. I.; Pereira, L. M. C.; Torne, J.; Vega, L. F. Polar Soft-SAFT: Theory and Comparison with Molecular Simulations and Experimental Data of Pure Polar Fluids. *Phys. Chem. Chem. Phys.* **2020**, *22* (23), 13171–13191.
- (75) Llovel, F.; Vega, L. F. Prediction of Thermodynamic Derivative Properties of Pure Fluids through the Soft-SAFT Equation of State. *J. Phys. Chem. B* **2006**, *110* (23), 11427–11437.
- (76) Llovel, F.; Peters, C. J.; Vega, L. F. Second-Order Thermodynamic Derivative Properties of Selected Mixtures by the Soft-SAFT Equation of State. *Fluid Phase Equilib.* **2006**, *248* (2), 115–122.
- (77) Colina, C. M.; Turrens, L. F.; Gubbins, K. E.; Olivera-Fuentes, C.; Vega, L. F. Predictions of the Joule - Thomson Inversion Curve for the n-Alkane Series and Carbon Dioxide from the Soft-SAFT Equation of State. *Ind. Eng. Chem. Res.* **2002**, *41* (5), 1069–1075.
- (78) DIPPR 801 Database - Design Institute for Physical Properties of the American Institute of Chemical Engineers- (Computer Software); DIPPR, 2017.
- (79) Allal, A.; Moha-ouchane, M.; Boned, C. A New Free Volume Model for Dynamic Viscosity and Density of Dense Fluids versus Pressure and Temperature. *Phys. Chem. Liq.* **2006**, *39* (1), 1–30.
- (80) TURBOMOLE Quantum Chemistry, BIOVIA - Dassault Systèmes, 2022 <https://www.3ds.com/products-services/biovia/products/molecular-modeling-simulation/solvation-chemistry/turbomole/>. (accessed January 4, 2022).
- (81) Canbolat, A. S.; Bademlioglu, A. H.; Arslanoglu, N.; Kaynakli, O. Performance Optimization of Absorption Refrigeration Systems Using Taguchi, ANOVA and Grey Relational Analysis Methods. *J. Cleaner Prod.* **2019**, *229*, 874–885.

- (82) Bademlioglu, A. H.; Canbolat, A. S.; Kaynakli, O. Multi-Objective Optimization of Parameters Affecting Organic Rankine Cycle Performance Characteristics with Taguchi-Grey Relational Analysis. *Renewable Sustainable Energy Rev.* **2020**, *117*, No. 109483.
- (83) Hanine, M.; Boutkhoun, O.; Tikniouine, A.; Agouti, T. Application of an Integrated Multi-Criteria Decision Making AHP-TOPSIS Methodology for ETL Software Selection. *SpringerPlus* **2016**, *5* (1), No. 263, DOI: 10.1186/s40064-016-1888-z.
- (84) Pàmies, J. C. Bulk and Interfacial Properties of Chain Fluids: A Molecular Modelling Approach, Ph.D. Thesis; Universitat Rovira i Virgili: Tarragona, Spain, 2004.
- (85) Mota-Martinez, M. T.; Hallett, J. P.; Mac Dowell, N. Solvent Selection and Design for CO₂ Capture—How We Might Have Been Missing the Point. *Sustainable Energy Fuels* **2017**, *1*, 2078.
- (86) Olajire, A. A. CO₂ Capture and Separation Technologies for End-of-Pipe Applications - A Review. *Energy* **2010**, *35* (6), 2610–2628.
- (87) Rayer, A. V.; Henni, A.; Tontiwachwuthikul, P. Molar Heat Capacities of Solvents Used in CO₂ Capture: A Group Additivity and Molecular Connectivity Analysis. *Can. J. Chem. Eng.* **2012**, *90* (2), 367–376.
- (88) Coulier, Y.; Ballerat-Busserolles, K.; Mesones, J.; Lowe, A.; Coxam, J. Y. Excess Molar Enthalpies and Heat Capacities of {2-Methylpiperidine-Water} and {N-Methylpiperidine-Water} Systems of Low to Moderate Amine Compositions. *J. Chem. Eng. Data* **2015**, *60* (6), 1563–1571.
- (89) Efimova, A. A.; Emel'yanenko, V. N.; Verevkin, S. P.; Chernyak, Y. Vapour Pressure and Enthalpy of Vaporization of Aliphatic Poly-Amines. *J. Chem. Thermodyn.* **2010**, *42* (3), 330–336.
- (90) Biotechnology, S. C. Material Safety Data Sheet 2019.
- (91) Toky Chemical Industry (TCI). TCI Chemicals. <https://www.tcichemicals.com/JP/en>.
- (92) Villarroel, J. A.; Palma-Cando, A.; Viloria, A.; Ricaurte, M. Kinetic and Thermodynamic Analysis of High-Pressure CO₂ Capture Using Ethylenediamine: Experimental Study and Modeling. *Energies* **2021**, *14* (20), No. 6822, DOI: 10.3390/en14206822.
- (93) Mazari, S. A.; Abro, R.; Bhutto, A. W.; Saeed, I. M.; Ali, B. S.; Jan, B. M.; Ghalib, L.; Ahmed, M.; Mubarak, N. M. Thermal Degradation Kinetics of Morpholine for Carbon Dioxide Capture. *J. Environ. Chem. Eng.* **2020**, *8* (3), No. 103814.